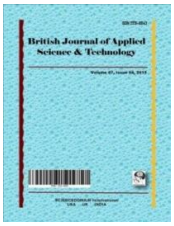

*British Journal of Applied Science & Technology*
*10(2): 1-11, 2015, Article no.BJAST.17442*
*ISSN: 2231-0843*

**SCIENCEDOMAIN** *international*
www.sciencedomain.org

# A Three Dimensional Finite Element Analysis for Contact Stress and Fatigue near the Fir-Tree Region in a Gas Turbine Blade

**Ganesh R. Navad[1], Narasimha Marakala[1], K. Vasudeva Karanth[2] and N. Yagnesh Sharma[2*]**

*[1]Department of Mechanical Engineering, NMAM Institute of Technology, Nitte, India.*
*[2]Department of Mechanical and Manufacturing Engineering, Manipal Institute of Technology, Manipal, India.*

***Authors' contributions***

*This work was carried out in collaboration between all authors. All authors read and approved the final manuscript.*

***Article Information***

DOI: 10.9734/BJAST/2015/17442
Editor(s):
(1) Grzegorz Golanski, Institute of Materials Engineering, Czestochowa University of Technology, Poland.
Reviewers:
(1) Anonymous, Uttar Pradesh Technical University, India.
(2) Anonymous, St. John's University, New York.
(3) Fang Wang, Faculty of Materials and Energy, Southwest University, China.
Complete Peer review History: http://sciencedomain.org/review-history/9817

***Original Research Article***

***Received 13th March 2015***
***Accepted 4th May 2015***
***Published 18th June 2015***

## ABSTRACT

In this work an attempt is made to simulate the life of a rotating element subjected to the phenomenon of fatigue fretting using finite element analysis. A numerical model is being proposed to analyse the fretting failure phenomenon. The model explores the physics of the problem with a view to capture micro slip at the interface between the root and the disc. Some of the parameters that affect fretting are dissimilar material component types, kinds of fit, geometry of the mating part etc. The effect of these parameters on the extent of fretting is being analysed using the commercial finite element tool ANSYS. This will enable one to gauge failure criterion of the part to be designed under different cyclic loading conditions subjected to fatigue fretting failure. It is found out from the present analysis that the bottom tooth of the fir tree structure experiences the maximum stress induced at the interface. Also the stress increases non-linearly as the speed increases. As the flank angle is increased, the fatigue life at higher speeds decreases. Also the equivalent stress decreases as the number of teeth increases.

**Corresponding author: E-mail: nysharma@hotmail.com;*

*Keywords: Fatigue; finite element analysis; fir tree, contact stresses; gas turbine blade.*

## 1. INTRODUCTION

Gas turbines play a very vital role in the energy domain, being the essential prime movers of energy generation in both moving and stationary power generating units. Typically gas turbines have very high temperature and pressure apart from being high-speed engines. This leads to design complexities such as thermal overruns and structural deformations. Thus the design of the gas turbine requires careful considerations of the above-mentioned factors. Even when due diligence is given to the above considerations regarding the design of the gas turbines, there is yet another important phenomenon that occurs in a gas turbine blade called “fretting” which occurs between two surfaces having oscillatory relative motion of small amplitude and with low sliding velocity (5 mm/s). This alternating movement with amplitude of less than 150 μm causes micro slip at the interface of the blade and the disc and hence the life of the blades is decreased drastically.

The mechanical integrity of aero engine turbine discs and attached blades is crucial to the operational safety and service life of gas turbine engines. Contact stresses, interface conditions (friction, surface roughness, residual stress), and the detailed geometry of the joint determine the severity of the resulting stress field and the magnitude of fatigue fretting. These thermo mechanical stresses do not remain constant but vary during a flight. It is generally accepted that fretting initiated fatigue cracks are due to intermittent high-frequency engine resonance and load fluctuations resulting from a change in engine speed or power requirements.

A three dimensional finite element analysis is required to capture the stresses induced due to fretting phenomenon. In the present analysis, the objective is to maximize the fatigue life of aero engine turbine blades. The analysis is carried out to predict the life of the blade-disc assembly taking centrifugal loading conditions into effect.

Aero engine turbine discs basically have three critical regions for which lifetime certification is necessary: (i) the fir-tree rim region, (ii) the assembly holes or weld areas, and (iii) the hub region [1]. The loads associated with these regions are the self-generated centrifugal forces of the disc and associated blades, the bending loads due to the gas pressure, and thermal loads. The joint between a turbine blade and the disc represents the most critical load path within that assembly. In the majority of cases, cracks are generally initiated in the fir-tree rim region due to the fretting action at the blade disc interface [2].

The stress analysis of the fir-tree region of aero engine discs has received some attention [3,4]. The theory of finite element formulation of two bodies in contact is discussed. The effect of blade and disc clearance upon the stress field using a two-dimensional FE model was investigated. The coefficient of friction was shown to have a slight effect on both the magnitude of maximum fillet stresses as well as the distribution of average loads on the teeth flanks. Clearance changes revealed more significant effects on the stress field than those of contact friction.

A variety of experimental stress analysis has been conducted [5] in three-dimensional photo-elastic specimens for dovetail skew geometries [6]. The experimental data suggested that the stress concentration factors were shown to increase with the skew angle defining the dovetail disc groove.

The scope of the current study is to obtain the fatigue fretting behaviour of a turbine blade at the fir tree interface when subjected to centrifugal loads. An attempt is made to establish a relationship between the different parameters affecting the fatigue life of the blade.

## 2. NUMERICAL MODELLING

### 2.1 Geometrical Modelling

An aero engine blade-disc assembly with a fir-tree structure is chosen for the analysis [7]. The nomenclature and specifications of the model are as shown in Fig. 2.1. The detailed specifications of the model created are shown in Table 2.1.

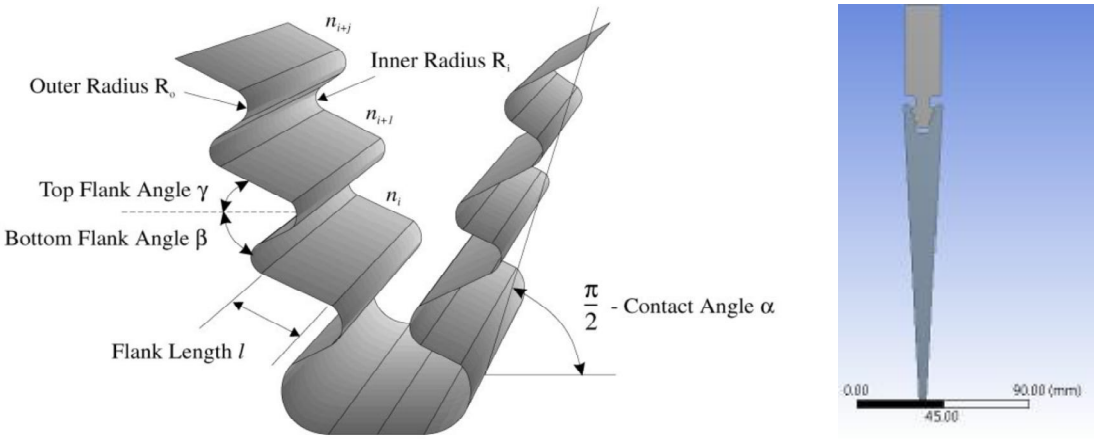


**Fig. 2.1. Nomenclature of fir tree root [5] and the geometrical model developed using ANSYS Workbench 14.5**

## 2.2 Assumptions used in the Analysis

The following assumptions are made for the present analysis

- A steady state non-linear structural analysis is adopted
- The analysis is restricted to within the elastic range of operations
- Centrifugal load being the major cause for failure is the only load that is considered in the analysis.
- Thermal effects on gas turbine blades are not considered in the present analysis.
- Coriolis forces caused due to relative motion of the fluid with respect to the rotating blade is assumed to be insignificant as evident from the literature review.

**Table 2.1. Detailed specifications of the model**

| Model Parameters | Value |
|---|---|
| Outer Radius ($R_o$) | 0.6833 mm |
| Inner Radius ($R_i$) | 0.5207 mm |
| Top flank angle ($\gamma$) | 40° |
| Bottom flank angle ($\beta$) | 40° |
| Contact angle ($\alpha$) | 15° |
| Number of teeth ($n_i$) | 3 |
| Flank length ($l$) | 3.556 mm |
| Inner radius of the disc ($a$) | 31.75 mm |
| Outer radius of the disc | 190.5 mm |

## 2.3 Parametric variables for the Analysis

The parameters of the fir tree are changed in order to obtain the variation of stresses. Some of the parameters that are changed are

- Contact angle (α)
- Number of teeth ($n_i$)
- Flank angles (β and γ)

## 2.4 Material Data for INCONEL 720

Material properties used for modelling the blade and the disc are that of a Nickel alloy namely INCONEL 720. The material has a modulus of elasticity of 220 GPa, a poisson's ratio of 0.29 and density of 8510 kg/m$^3$. The material is particularly selected because of its high resistance to creep and fatigue [8].

## 2.5 Mesh and Grid Independence Test

An initial coarse meshing scheme is adopted in the preliminary analysis to generate the computational model domain. The output result generated from this preliminary analysis is plotted for one of the important design outputs i.e. Von Mises equivalent stress along the thickness of the blade as it is an essential parameter to assess the strength of the tooth in the fir tree domain. The reference mesh created is illustrated in Fig. 2.3(a) where the elements are uniformly distributed with a minimum size of 0.25 mm. However the uniform mesh for the whole model results in the drastic increase in computational time to obtain the results. Hence the mesh is refined (Fig. 2.3 b) as per the stress concentration so as to obtain a balance between getting an accurate solution and keeping the computational time low.

A numerical model needs to have consistent results for any parametric variation corresponding to an optimal number of nodes

and elements. Hence it is necessary to model the computational domain with a graded increase of nodes and corresponding number of elements. The numerical model is tested for 4 different grades of mesh density with model A being coarse with 489,997 nodes and 111,060 elements and model D being finer model with 2,943,160 nodes and 696,900 elements. The grid independence test is carried out for the principle variable von mises equivalent stress which is plotted along the thickness of the disc. By comparison of the variation of the von mises equivalent stress among the four models it is seen that models C and D show near convergence trend in variation. Hence considering the computational cost and time, model C with 1,863,248 nodes and 437,200 elements is adopted for numerical modelling.

**Table 2.2. Mesh densities of the models used for grid independence test**

| Model | Elements | Nodes |
|---|---|---|
| Model A | 111,060 | 489,997 |
| Model B | 246,990 | 1,065,773 |
| Model C | 437,200 | 1,863,248 |
| Model D | 696,900 | 2,943,160 |

## 2.6 Boundary Conditions

- Frictionless support for the inner face of the disc to constrain and provide an axis of rotation for the blade disc assembly.
- Rotational Velocity of the disc – 1000 RPM simulating the centrifugal load applied.
- Restricting the displacement of the side faces normal to its plane.
- Cyclic symmetry of the disc.

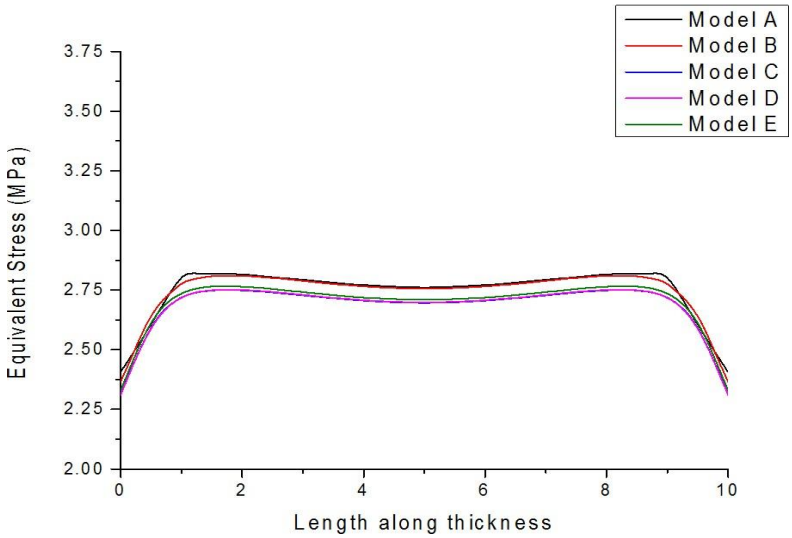


**Fig. 2.2. Plot of equivalent stress along the thickness of the disc**

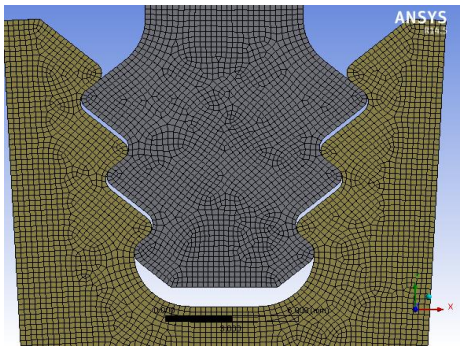


**Fig 2.3(a). Uniform hex mesh of the assembly**

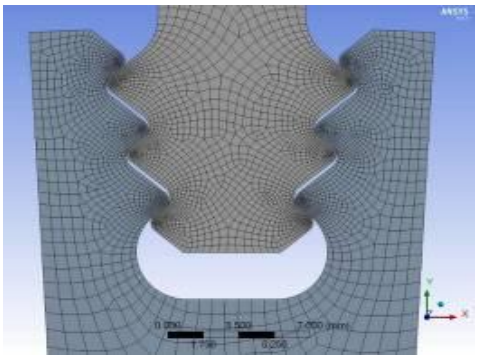

**Fig 2.3(b). Hex mesh having a finer mesh at the contact faces**

## 2.7 Contact Surface Formulation

The contacting surfaces in the fir-tree region were modelled using contact surface elements. These elements allow for the modelling of gap and friction conditions at the interface [9]. Two methods of satisfying non-linear contact conditions are available: a penalty method and a combined penalty Lagrange multiplier method also known as Augmented Lagrange method. Both methods involve the use of user defined parameters: normal and tangential stiffness, $K_n$ and $K_s$ respectively. These stiffness factors play a major role in governing the convergence and accuracy of the solution. The values for stiffness were chosen such that the criteria of minimum interpenetration and convergence were satisfied. The minimum interpenetration was selected to be 5% of the smallest element size. Furthermore, the solution was accepted if convergence between two successive iterations did not exceed 2%. The interface between the disc and the blade is of much importance since the stresses generated will be at the maximum in this region. The assigned contact and target faces are highlighted as red and blue respectively as shown in Fig. 2.4.

## 2.8 Validation of the Numerical Model

The validation of the numerical model was carried out by comparing the results of the present study with the one available in literature [7] and is illustrated in the plot shown in Fig. 2.5. The stresses induced along the periphery of a tooth in the fir tree are compared with the results from photo-elastic model of the fir tree tooth from an experimental model. The photo-elastic model was created by stress-freezing experiments conducted using a photoelastic turbine blade-disc assembly with the material made of Araldite CT200 epoxy and the spin speed of 360 RPM was selected for stress freezing process.

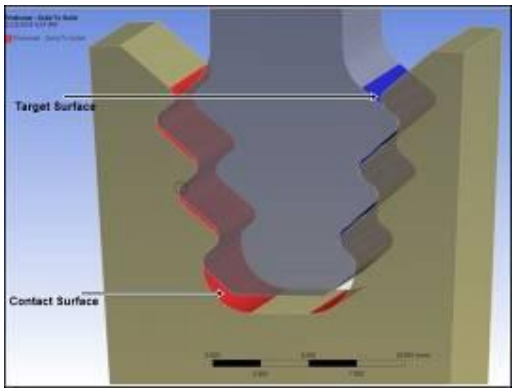


**Fig. 2.4. Contact and target faces at the blade disc interface**

**Table 2.3. Contact formulation details**

| Parameter | Value |
|---|---|
| Type of contact | Frictional |
| Coefficient of friction | 0.2 |
| Contact algorithm | Augmented Lagrange's Method |
| Contact behavior | Symmetric |
| Normal Stiffness | $5.2750 \times 10^8$ N/m |
| Tangential Stiffness | 1020 N/m |

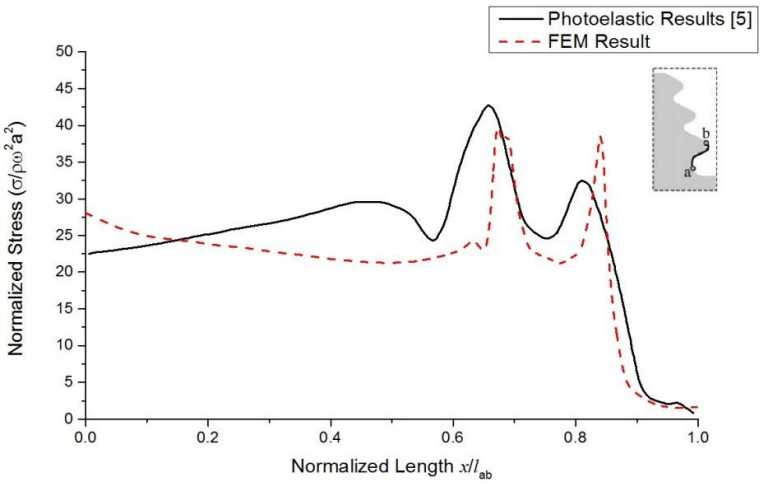


**Fig. 2.5. Validation graph of normalized length vs Normalized stress for photo-elastic maximum shear stress contours and Finite Element predictions**

### 2.9 Normalization of Stresses

In order to obtain a dimensionless variable for easy scalability of the results, the finite element results which are obtained in terms of MPa were normalized by a factor of $\rho\omega^2a^2$ [7]. The normalized factor obtained is 12.2 kPa.

### 2.10 Determination of Fatigue Life

The important part in determining the amount of fatigue fretting lies in the methods used for calculating the fatigue life [10,11]. In the current scenario, as the number of cycles of loading and unloading are high, hence the method used for calculating the fatigue life is stress based approach. The loading was applied from no load to full load and the life cycles are based on this number. Also The Goodman mean stress theory was used to predict the life of the blade disc assembly [8].

## 3. RESULTS AND DISCUSSION

### 3.1 Effect of Contact Angle (α)

Fig. 3.1 shows the contour plots for the case for various contact angles. As the contact angle increases the equivalent stress increases and the stress distribution decreases in the fir tree region.

It appears as a stress concentration region at the contact point between the blade and the disc. This is due to the fact that as the contact angle is increased, the contact area between the disc and the blade also decreases leading to higher stresses in those regions.

The maximum load bearing is by the disc owing to the fact that the blade is supported by the disc leading to higher stresses in the load bearing region of the disc.

Fig. 3.2 shows a bar graph showing the variation of normalized equivalent and shear stresses with respect to contact angle α. It is found that there is a sudden spurt in the value of the stresses for the case with a contact angle of 22.5° which is due to geometric distortion at the teeth of the blade and disc interface.

Fig. 3.3 shows the stresses generated along the thickness of the blade. The graph reveals that the stresses vary along the thickness with stress being higher at the edges than at the center. This bucket shaped formation of stress variation is due to factors such as the non-linear contact formulation and slippage occurring between the faces of the blade and the disc. Comparing the linear stresses along the thickness for the 4 models indicate a higher stress magnitude for the model with a contact angle of 22.5° and the least for the one with 15° contact angle.

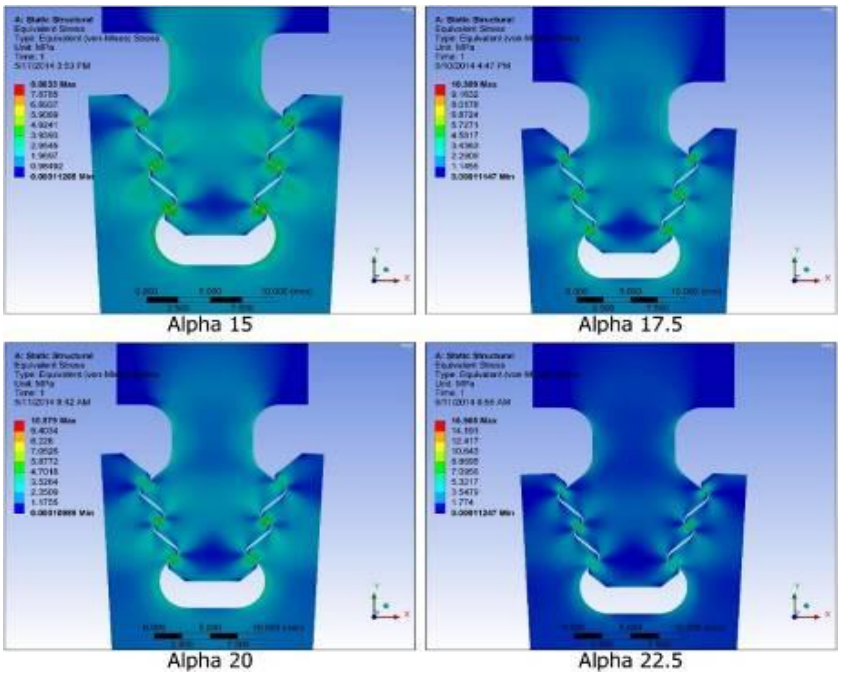


**Fig. 3.1. Equivalent stress contour plots of varying alpha angles**

Fig. 3.3 shows the stresses generated along the thickness of the blade. The graph reveals that the stresses vary along the thickness with stress being higher at the edges than at the center. This bucket shaped formation of stress variation is due to factors such as the non-linear contact formulation and slippage occurring between the faces of the blade and the disc. Comparing the linear stresses along the thickness for the 4 models indicate a higher stress magnitude for the model with a contact angle of 22.5° and the least for the one with $15^0$ contact angle.

Plot of the fatigue life of the four models against the rotor speed illustrated in Fig. 3.4 indicates that the model with a 15° contact angle exhibits a higher resistance to failure. Considering a threshold of $10^8$ cycles, the maximum speed attainable by the model with 15° contact angle is much higher than the other models.

## 3.2 Effect of Number of Teeth ($n_i$)

From the comparison of the equivalent stress contour plots for the models with 3, 4 and 5 teeth as shown in Fig. 3.5, it is observed that as the number of teeth increases, the equivalent stress decreases progressively. The plot of equivalent and shear stress for the 3 models are illustrated in Fig. 3.6. This can be attributed to the fact that increasing the number of teeth also increases the contact area in the fir tree region. Hence the induced stresses are distributed amongst the teeth and these stresses are relatively low as the number of teeth is increased.

The increase in number of teeth will affect the stress concentration thereby reducing it and the stresses are distributed along the volume of the fir tree region.

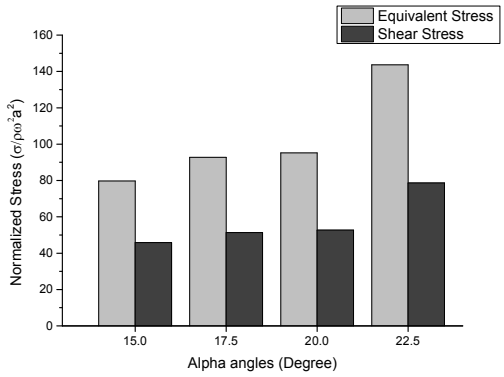


**Fig. 3.2. Graph of normalized Von Mises and shear stress with contact angle (α)**

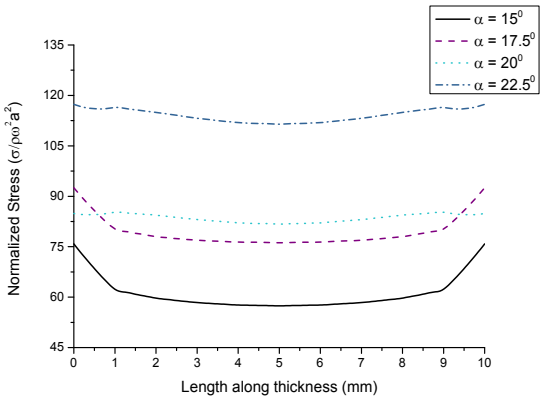


**Fig. 3.3. Linearized stress along the thickness for varying alpha angles**

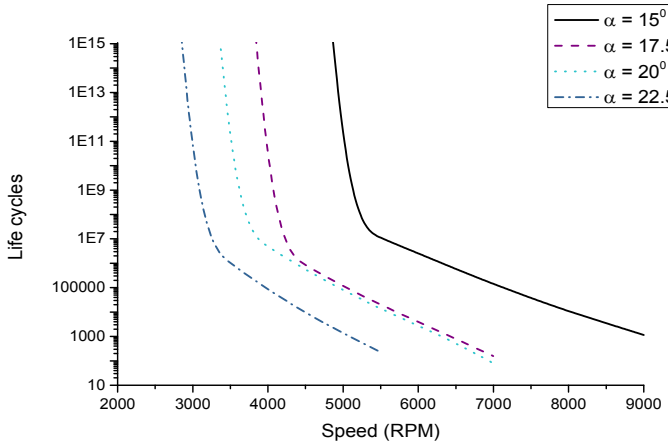


**Fig. 3.4. Fatigue life of the assembly vs speed for different alpha angles**

From the Fig. 3.7 the linearized stress variation along the thickness show a marked change from 3 teeth to 5 teeth. Whereas the stress variation shows significant change along the thickness for 3 teeth fir tree, the stress variation for 4 teeth and 5 teeth show a lower but nearly flat profile. This is because of the better load bearing capacity for higher number of teeth and hence lower stresses in higher teeth fir tree. However a weighted average of the stresses along the thickness reveals that there is an optimum for 4 teeth profile with lower average stresses for the 4 teeth model. This can be inferred from Fig. 3.7 as there is an inflection between the profiles of 4 and 5 teeth stress distribution. From the fatigue life vs speed chart as shown in Fig. 3.8, it is observed that for $10^8$ cycles the models with 4 and 5 teeth exhibit the same resistance to fatigue since the maximum speed attainable by the two models are approximately similar.

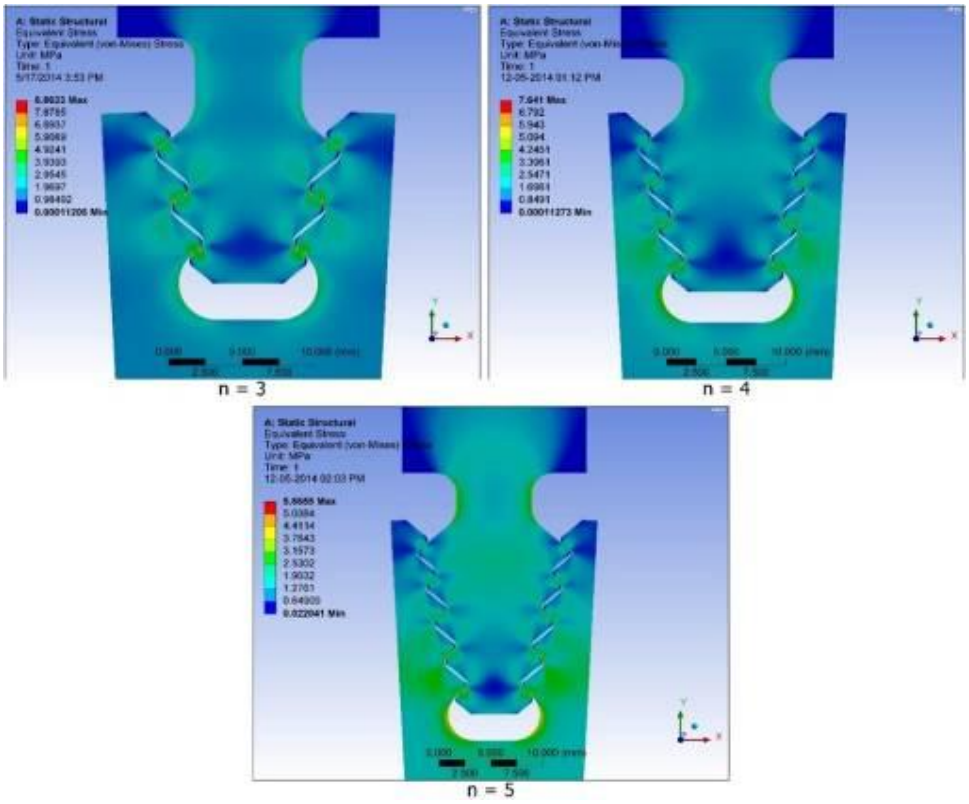


**Fig. 3.5. Equivalent stress contour plots for varying number of teeth**

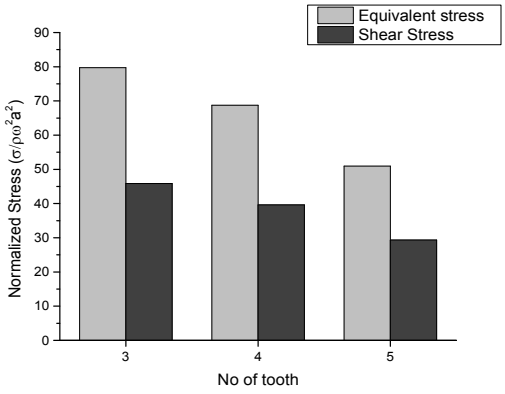


**Fig. 3.6. Graph of normalized Von Mises and shear stress with no of tooth ($n_i$)**

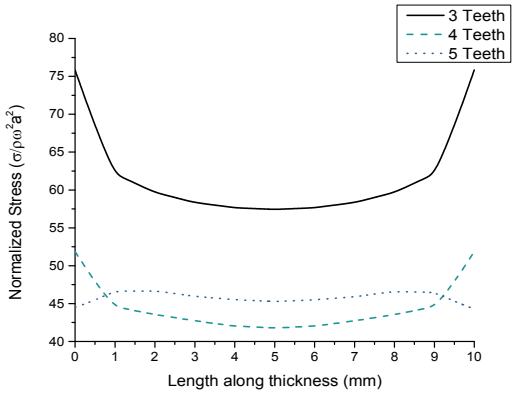


**Fig. 3.7. Linearized stress along the thickness for varying number of teeth**

### 3.3 Effect of Top and Bottom Flank Angles

It is found from stress contour plot (Fig. 3.9) and bar graph of equivalent and shear stress for the 3 models (Fig. 3.10) that there is negligible variation in the stress distribution due to the variation in top and bottom flank angles. Hence it can be concluded that the top and bottom flank angles do not have significant role in the induced stresses at the fir tree region. The increase or decrease in top or bottom flank angles results in a blunt or sharp tooth. Therefore the amount of slip varies as the assembly is subjected to centrifugal load.

From the fatigue life vs speed chart as shown in Fig. 3.12, it is observed that for $10^8$ cycles the two models which has 30° and 50° top and bottom flank angles exhibit the same resistance to fatigue irrespective of the amount of slippage. But the resistance to fatigue of the same is higher than the model with equal top and bottom flank angles.

The plot of linearized stress along the thickness as illustrated in Fig. 3.11 indicates that the model with bottom flank angle below 30° produces high stresses along the thickness. Therefore it can be assumed that any tooth angle less than 40° produces unfavourable results. It is also observed that the stress does not vary significantly by the increase of flank angle.

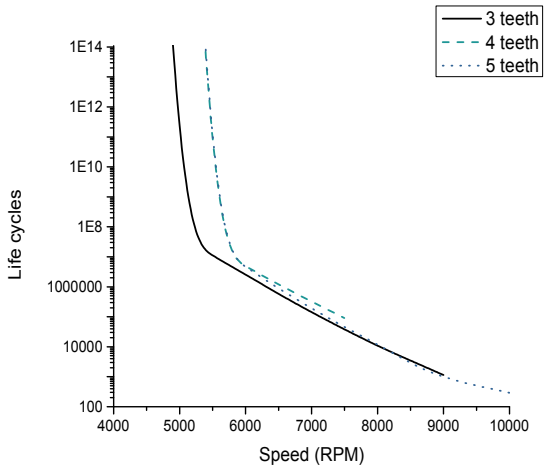


**Fig. 3.8. Fatigue life of the assembly vs speed for varying number of teeth**

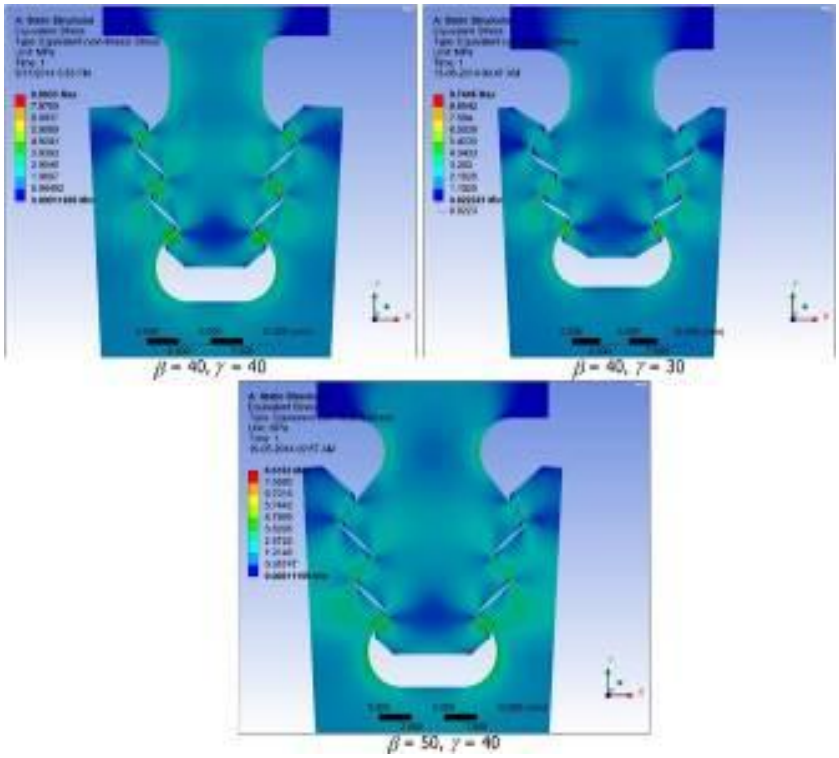


**Fig. 3.9. Equivalent stress contour plots for varying top and bottom flank angles**

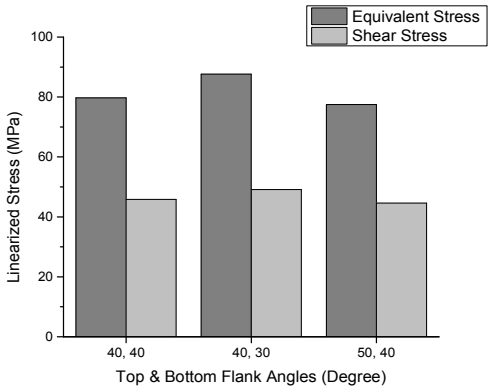


**Fig. 3.10. Graph of normalized Von Mises and shear stress with flank angles**

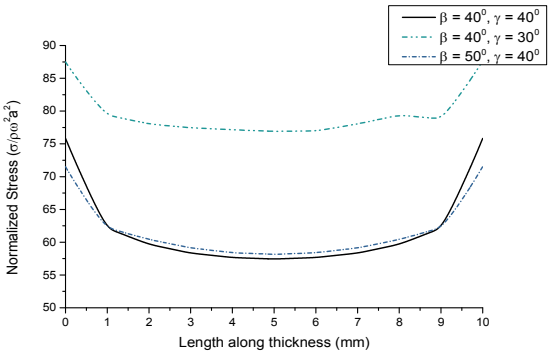


**Fig. 3.11. Linearized stress along the thickness for different combinations of top and bottom flank angles**

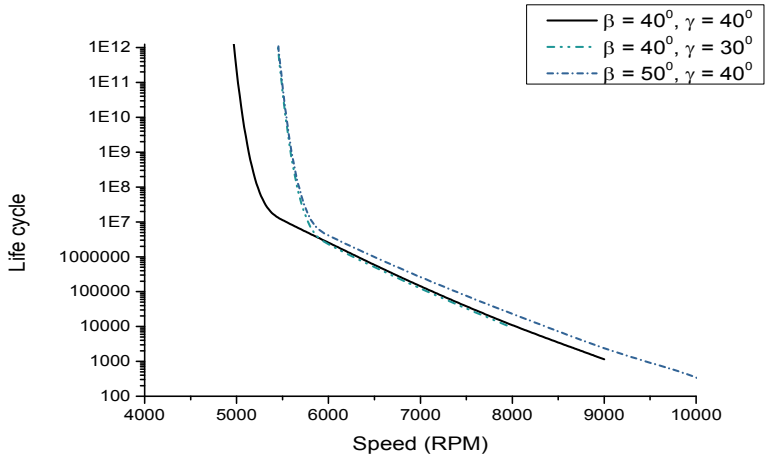


**Fig. 3.12. Fatigue life of the assembly vs speed for different combinations of flank angles**

## 4. CONCLUSION

The following important conclusions were derived from the parametric study of fatigue fretting in rotating structures with interference fitted components using ANSYS:

1. It was observed from the study that the equivalent stress increases from the bottom tooth to the top tooth. Further, the plot of normalized stress along the periphery of the tooth profile from bottom to top showed a variation with bottom tooth exhibiting a higher peak compared to the top tooth. The tooth trough experienced relatively no stress due to the gap (clearance) between the blade and disc.
2. As the contact angle was increased, the stress concentration also increased proportionately.
3. The fatigue life for different rotor speed indicated that the model with a 15° contact angle exhibited a higher resistance to failure. Considering a threshold of $10^8$ cycles, the maximum speed attainable by the model with 15° contact angle was 5200 rpm as compared to 4250 rpm of 17.5°, 3700 rpm of 20° and 3000 rpm of 22.5° angle of contact.
4. It was observed that as the number of teeth increases, the equivalent stress decreased progressively. The increase in number of teeth affects the stress concentration, thereby reducing it and the stresses were distributed along the surface of the fir tree region.

## COMPETING INTERESTS

Authors have declared that no competing interests exist.

## REFERENCES


1. Meguid SA. Engineering fracture mechanics, 1st ed. Elsevier Applied Science, London; 1988.
2. Papanikos P, Meguid SA. Theoretical and experimental studies of fretting-initiated fatigue failure of aeroengine compressor discs. Fatigue Fract Eng. Mat. Struct. 1994;539–550.
3. Chan SK, Tuba IS. A finite element method for contact problems of solid bodies – Part I. Theory and Validation, International Journal of Mechanical Sciences. 1971;615-625.
4. Chan SK, Tuba IS. A finite element method for contact problems of solid bodies - Part II: applications to turbine blade fastenings, International Journal of Mechanical Sciences. 1971;627–639.
5. Songa W, Andy Keanea, Janet Reesb, Atul Bhaskara, Steven Bagnallb. Turbine blade fir-tree root design optimization using intelligent CAD and finite element analysis. Computers & Structures. 2002;80(24): 1853–1867.
6. Murthy H, Daniel B Gracia, John F Matlik, Thomas N Farris, Fretting fatigue of single crystal/polycrystalline nickel subjected to blade/disk contact loading. Acta Astronautica. 2005;57(1):1–9.
7. Meguid SA, et al. Finite element analysis of fir-tree region in turbine discs, Finite Elements in Analysis and Design. 2000; 35(4):305–317.
8. Tiago de Oliveira Vale, Gustavo da Costa Villar, João Carlos Menezes. Methodology for structural integrity analysis of gas turbine blades. Journal of Aerospace Technology and Management. 2012;51–60.
9. Reza Hojjati, Magd Abdel Wahab, Eugenio Giner, Mohamad Sabsabi. Numerical estimation of fretting fatigue lifetime using damage and fracture mechanics, Tribology Letters. 2013;52(1):11–25.
10. Poursaeidi E, Mohammadi MR. Failure analysis of lock-pin in a gas turbine engine. Journal of Engineering Failure Analysis. 2008;847–855.
11. Jianfu Hou, Bryon J Wicks, Ross A Antoniou. An investigation of fatigue failures of turbine blades in a gas turbine engine by mechanical analysis. Journal of Engineering Failure Analysis. 2002;201–211.




*Peer-review history:*
*The peer review history for this paper can be accessed here:*
*http://sciencedomain.org/review-history/9817*